ACS APPLIED MATERIALS & INTERFACES

Research Article

www.acsami.org

Facile Preparation Route for Nanostructured Composites: Surface-Initiated Ring-Opening Polymerization of ε-Caprolactone from High-Surface-Area Nanopaper

Assya Boujemaoui,[†,‡] Linn Carlsson,[†] Eva Malmström,[†] Mohammed Lahcini,[‡] Lars Berglund,[†,§] Houssine Sehaqui,*[,†,⊥] and Anna Carlmark*[,†]

[†]KTH Royal Institute of Technology, School of Chemical Science and Engineering, Fibre and Polymer Technology, and [§]Wallenberg Wood Science Center, Teknikringen 56, SE-100 44 Stockholm, Sweden

[‡]Laboratory of Organometallic and Macromolecular Chemistry - Composites Materials, Faculty of Sciences and Technologies, Cadi Ayyad University, Avenue Abdelkrim Elkhattabi, B.P. 549, 40000 Marrakech, Morocco

Supporting Information

ABSTRACT: In this work, highly porous nanopaper, i.e., sheets of papers made from non-aggregated nanofibrillated cellulose (NFC), have been surface-grafted with poly(ε-caprolactone) (PCL) by surface-initiated ring-opening polymerization (SI-ROP). The nanopaper has exceptionally high surface area (~300 m^2/g). The "grafting from" of the nanopapers was compared to "grafting from" of cellulose in the form of filter paper, and in both cases either titanium *n*-butoxide ($Ti(On\text{-}Bu)_4$) or tin octoate ($Sn(Oct)_2$) was utilized as a catalyst. It was found that a high surface area leads to significantly higher amount of grafted PCL in the substrates when $Sn(Oct)_2$ was utilized as a catalyst. Up to 79 wt % PCL was successfully grafted onto the nanopapers as compared to filter paper where only 2−3 wt % PCL was grafted. However, utilizing $Ti(On\text{-}Bu)_4$ this effect was not seen and the grafted amount was essentially similar, irrespectively of surface area. The mechanical properties of the grafted nanopaper proved to be superior to those of pure PCL films, especially at elevated temperatures. The present bottom-up preparation route of NFC-based composites allows high NFC content and provides excellent nanostructural control. This is an important advantage compared with some existing preparation routes where dispersion of the filler in the matrix is challenging.

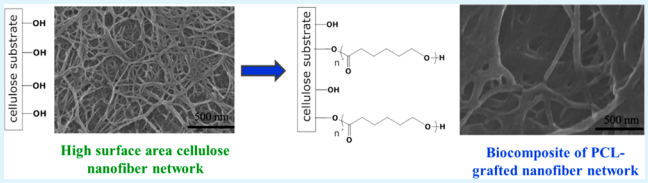

KEYWORDS: *ring-opening polymerization, nanofibrillated cellulose, nanopaper, surface grafting, high surface area*

INTRODUCTION

Bionanocomposites have gained increasing interest over the last decades due to their improved mechanical and thermal properties, and to their environmentally friendly character. In this context, researchers have been interested to use cellulose to reinforce polymeric matrices since it is a renewable, natural, abundant and biodegradable resource.[1] Several types of cellulose have been investigated as nanofiller, mainly nanofibrillated cellulose (NFC) and cellulose nanowhiskers (CW's), taking advantage of their high modulus and large surface area. NFC is composed of high aspect ratio cellulose nanofibrils obtained after mechanical disintegration of cellulose. CW's are obtained via acid hydrolysis of cellulose, meaning that the amorphous part is removed, and the remaining fibrils are rodlike. Nowadays, NFC disintegration is facilitated by the use of enzymatic[2] or chemical pretreatments,[3] or a combination of the two, so that the energy required for the mechanical disintegration is reduced and the fibrils obtained have a smaller diameter.

The major drawback of using cellulose as reinforcement for nonpolar polymer matrices is its hydrophilic character, which makes its incorporation and its adhesion to the matrix a difficult task. To overcome this, cellulose can be modified chemically, with low molecular weight compounds or by grafting polymers on its surface.[4−7] Poly(ε-caprolactone) (PCL) has previously been utilized for cellulose surface modification.[8−10] It is an interesting polymer since it is biocompatible and biodegradable. PCL is produced by ring-opening polymerization (ROP) of ε-caprolactone (ε-CL). Catalysts based on tin, especially tin octoate ($Sn(Oct)_2$), are undoubtedly the most widely used catalysts for the ROP of lactides and lactones and other cyclic esters due to their excellent performance and good thermostability. However, most tin compounds have a relatively high cytotoxicity[11] and require inert atmosphere[12] which increase the manufacturing cost. In this context, several metal-based catalysts with lower toxicity have been studied for the ROP of lactones and lactides.[13] Recently, Parssinen et al.[14] showed that titanium alkoxides allow ROP of ε-CL in air. The reactivity and the mechanism of titanium alkoxides catalysts were studied by Kricheldorf et al.[15] and Cayuela et al.[16] who concluded that these catalysts are composed of titanium with four ligands having similar reactivity and the proposed mechanism was

Received: March 27, 2012
Accepted: May 30, 2012
Published: May 30, 2012

coordination insertion of the catalyst to the monomer via its carbonyl group followed by ring-opening of the cyclic monomer and, furthermore, several coordination insertion steps lead to the PCL chain growth (Scheme 1). Titanium alkoxides have previously been utilized to successfully graft solid surfaces such as carbon nanotubes, starch and silica.[17,18]

Several studies have been reported on the grafting of ε-CL from cellulose substrates.[6,8,9,19−23] Cellulose is a hydroxyl functional polymer which means that it can act as an initiator for the surface-initiated grafting reaction of PCL without prior modification. In the case of NFC, obtained in the form of an aqueous suspension, the main challenge for ε-CL grafting is water removal, because the polymerization reaction is moisture-sensitive. Water can initiate the ROP and its presence leads to lower molecular weight compounds and decreased control of the polymerization. To remove water from NFC, solvent exchange into an organic solvent can be performed, but this is a tedious step. To circumvent this, Malmström et al.[21] dried NFC in air (according to a vacuum filtration and air drying method) rendering a dense NFC nanopaper, which was subsequently grafted with PCL. Recently, a nanopaper with high porosity and high surface area was developed by vacuum filtration and supercritical drying.[24] The nonagglomerated fibrils in this nanopaper result in a surface area as high as 300 m^2/g and this corresponds to a fibril diameter of 9 nm available for further functionalization (assuming a cylindrical model of the fibrils). Grafting from such nanopaper would be highly advantageous as the distribution of the PCL would not be restrained to the surface of the paper and grafting of fibrils and fibrils aggregate would be possible.

In a previous study, high NFC content in composites was found to increase strength, stiffness and toughness compared to the unfilled matrix.[25] It is generally challenging to prepare composite materials with high loading of nanofiller since the processing and nanofiller dispersion become difficult. Therefore, in the present study, we investigated the grafting of ε-CL on highly porous nanopaper, with a high surface area, via in situ SI-ROP of ε-CL using titanium butoxide or tin octoate as catalyst for the reaction. The resulting covalent bond between the substrate and the PCL should allow better stress transfer between the two components under moist conditions as the moisture uptake of the composites will be reduced. Reactions were also performed on conventional filter paper in order to study the grafting efficiency both on high and low surface area cellulose substrates using two different catalysts (tin based and titanium based). The objective was to develop a new method for preparation of NFC based nanocomposites composed of a PCL polymer matrix grafted onto a well dispersed and high surface area NFC network. This nanofibril network is a unique template for truly nanostructured composites, since only a limited amount of nanofibril agglomerates are present.[24] Characterization of the present material was performed by FT-IR, DSC, FE-SEM, dynamic vapor sorption analysis (DVS), BET specific surface area, and DMA measurements.

EXPERIMENTAL PROCEDURES

Materials. ε-Caprolactone (ε-CL) (Sigma-Aldrich, 99%) and benzyl alcohol (BnOH) were distilled over calcium hydride under reduced pressure prior to use. Titanium n-butoxide ($Ti(On\text{-}Bu)_4$), tin octoate ($Sn(Oct)_2$), tetrahydrofurane (THF) and methanol (MeOH) were purchased from Sigma-Aldrich and used as received without further purification. Filter paper (Whatman #1) was cut into pieces of 2.5 × 3 cm^2, washed with acetone and methanol and then dried in vacuum oven at 50 °C for 24 h prior to use. NFC aqueous suspension was prepared according to the enzymatic pretreatment method in which softwood sulphite pulp fibers were subjected to the hydrolytic action of endoglucanase at 50 °C then subjected to a high shear mechanical treatment in the microfluidizer.[2] From the NFC aqueous suspension, the high surface area nanopaper was prepared by vacuum filtering a 0.1% NFC suspension over 0.65 μm membrane until a strong "cake" was formed. This cake was then solvent exchanged to methanol and dried using supercritical CO_2 in a critical point dryer (Tousimis).

Surface-Initiated ROP of ε-CL from Nanopaper or Filter Paper Using $Ti(On\text{-}Bu)_4$. The monomer ε-CL (20.6 g, 181 mmol) and the cellulose substrate (filter paper or nanopaper) with a known weight were put into an E-flask equipped with a magnetic stirrer. A catalytic amount of the catalyst $Ti(On\text{-}Bu)_4$ (35.4 mg, 0.10 mmol, $DP_{(100\%conv)}$ = 451) was added and the mixture was degassed for 30 min to ensure dispersion of the catalyst into the cellulose substrates. The calculation of ratio monomer-to-catalyst which corresponds to the degree of polymerization for complete monomer conversion ($DP_{(100\%conv)}$), was performed according to the following equation:

$$DP_{(100\%conv)} = n(M)/4 \times n(cat)$$

Where $n(M)$ and $n(cat)$, respectively, are the number of moles of the monomer and the catalyst.

Thereafter, the E-flask was immersed in a preheated oil bath at 120 °C. Samples of the free forming polymer were continuously withdrawn for determination of the monomer conversion by ^1H NMR. After the reaction, the flask was cooled down by placing it in an ice bath and then THF was added to the mixture. The free (nonbonded) PCL was precipitated into cold methanol, filtrated, dried in vacuum oven at 50 °C and then characterized by SEC in THF. To remove the residual nongrafted PCL, the grafted cellulose substrate was ultrasonicated three times in 50 mL of THF for 10 min, and thereafter Soxhlet extracted for 24 h in THF. After Soxhlet extraction, the grafted filter paper was dried under vacuum for one night, whereas the grafted nanopaper was dried with supercritical CO_2 after being solvent exchanged to methanol.

Surface-Initiated ROP of ε-CL from Nanopaper or Filter Paper Using $Sn(Oct)_2$. ROP was conducted in an E-flask equipped with a magnetic stirrer in which the monomer ε-CL (20.6 g, 180.5 mmol) and filter paper (washed, dried and weighed prior to use) were added. The co-initiator benzyl alcohol (47.2 mg, 0.44 mmol, $r_{M/init}$ = 410) and the catalyst $Sn(Oct)_2$ (0.4 g, 2 wt % of ε-CL) were added to the reaction flask under argon flow. The calculation of ratio monomer-to-catalyst that corresponds to the degree of polymerization for complete monomer conversion, $DP_{(100\%conv)}$ was performed according to the following equation

$$DP_{(100\%conv)} = n(M)/n(init)$$

Where $n(M)$ and $n(init)$, respectively, are the number of moles of the monomer and the initiator.

Thereafter, the flask was degassed by 3 vacuum/argon cycles and then immersed in an oil bath preheated at 120 °C. The cellulose substrate and the unbound polymer were treated as described above.

Characterization. *Proton Nuclear Magnetic Resonance (^1H NMR).* ^1H-NMR was performed on a Bruker AM 400 at 400 MHz using $CDCl_3$ as solvent was used to determine the conversion of the nongrafted PCL. The solvent signal was used as an internal standard. The theoretical molecular weight ($M_{n,th}$) of the free PCL was estimated from the conversion (conv.) assessed by ^1H NMR. The conversion was calculated by the ratio of the signals at 4.05 ppm ($-CH_2O$-, polymer repeating unit) and 4.20 ppm ($-CH_2O-$, monomer). $M_{n,th}$ of PCL was calculated according to the following equation:

$$M_{n,th} = conv. \times M(\varepsilon\text{-CL}) \times DP_{(100\%conv)}$$

Where M(ε-CL) is the molar masse of ε-CL and $DP_{(100\%)}$ is the degree of polymerization for 100% monomer conversion.

Size Exclusion Chromatography (SEC). SEC on free PCL was performed using a Verotech PL-GPC 50 equipped with two PLgel 10 μm mixed D (300 × 7.5 mm) columns (Varian) and a PL-AS RT autosampler. $CHCl_3$ was used as the mobile phase (1.0 mL/min). The measurement was performed at 30 °C. Linear polystyrene standards were used to calibrate SEC apparatus, and toluene as flow rate marker. Cirrus GPC Software was used to assess data.

Fourier Transform-Infrared Spectroscopy (FT-IR). FT-IR was conducted on a Perkin-Elmer Spectrum 2000 FT-IR equipped with a MKII Golden Gate, Single Reflection ATR system from Specac Ltd., London, U.K. All spectra were normalized against a specific ATR crystal adsorption to enable comparison between the grafted cellulose substrates.

Dynamic Vapor Sorption (DVS). Moisture sorption measurements are made with a DVS, Dynamic Vapor Sorption (Surface Measurement Systems Limited, smsuk.co.uk). A micro balance and a moisture generation system are placed in an incubator keeping constant temperature. A sample ca. 10 mg is placed in the sample cup, and the weight, with a resolution of 0.1 μg, of the sample compared to the reference is registered while the relative humidity surrounding the cups is controlled. Samples were tested in the DVS at an average temperature of 32.6 °C. The moisture was set to 0, 25, 50, and 80% RH. A time of 1000 min was used at each step to ensure equilibrium in the material. The DVS sorption isotherm was calculated from an average of the last 4 min of each RH-step. The change in mass was calculated as the moisture ratio, i.e., the mass of the water in the sample divided by the dry weight of the sample.

Differential Scanning Calorimetry (DSC) Analysis. DSC was performed on a Mettler Toledo DSC 820 equipped with a Mettler Toledo Sample Robot TSO801RO calibrated using standard procedures with cooling and heating rate of 10 °C/min. The sample was heated to 150 °C and equilibrated for 3 min to erase any previous thermal history, and thereafter cooled to −30 °C. After equilibration (3 min) the sample was reheated to 150 °C. The degree of crystallization (X_C) was estimated from the crystallization transition according to the following calculation

$$X_c = \Delta H/(w \times \Delta H^0_{100})$$

Where ΔH is the heat of fusion of the sample, w is the weight fraction of PCL, and ΔH^0_{100} is the heat of fusion for a 100% crystalline PCL, the value used was fixed to 136.4 J/g according to the literature.[26]

Field-Emission Scanning Electron Microscopy (FE-SEM). The surface texture of the grafted and non-grafted cellulose substrates was observed by SEM using a Hitachi S-4800 equipped with a cold field-emission electron source. Images were captured for grafted cellulose substrates samples coated with graphite and gold−palladium using Agar HR sputter coaters (ca. 5 nm).

Specific Surface Area (BET) and Pore Size Distribution. The Brunauer−Emmett−Teller (BET)[27] surface area was determined by N_2 physisorption using a Micromeritics ASAP 2020 automated system. The porous nanopaper (and filter paper) sample was first degassed in the Micromeritics ASAP 2020 at 115 °C for 4 h prior to the analysis followed by N_2 adsorption at −196 °C. BET analysis was carried out for a relative vapor pressure of 0.01−0.3 at −196 °C. Pore size distribution was determined from N_2 desorption at relative vapor pressure of 0.01−0.99 following a BJH model that assumes a cylindrical shape of the pores.[28]

Density and Porosity Measurements. The density of the materials was determined by measuring their weight and dividing it by their volume. The volume was calculated from the thickness of the material (determined by a digital calliper) and its area.

Porosity for the cellulose substrates is deduced from the density of the substrate by taking 1460 kg m^{-3} as density of cellulose[29] using the formula

$$\text{porosity} = 1 - \frac{\rho_{\text{substrate}}}{\rho_{\text{cellulose}}} \quad (1)$$

Porosity of the grafted substrates is calculated from their densities and compositions according to the following equations

$$\text{porosity} = 1 - \frac{\rho_{\text{grafted\_substrate}}}{\rho_{\text{solid}}} \quad (2)$$

$$\rho_{\text{solid}} = \frac{1}{W_{\text{NFC}}/\rho_{\text{cellulose}} + W_{\text{PCL}}/\rho_{\text{PCL}}} \quad (3)$$

W_{NFC} and W_{PCL} are the respective weight fractions of NFC and PCL in the grafted substrates. ρ_{PCL} is the density of PCL taken as 1100 kg/m^3.[30]

Dynamic Mechanical Analysis (DMA). DMA was carried out on a Q800 DMA analyzer (TA Instruments, USA) in tension mode. Samples were cut to pieces of 5 mm in width and the distance between clamps was around 10 mm. The sample was cooled to −50 °C and equilibrated for 1 min. After equilibration the sample was reheated to 300 °C with heating rate of 5 °C min^{-1} and a frequency of 1 Hz.

An empirical equation, often termed the Tsai-Pagano model,[31] was used to estimate theoretical modulus of the composites (E_c)

$$E_c = \frac{3}{8}E_L + \frac{5}{8}E_T \quad (4)$$

Where E_L is longitudinal composite modulus for nanofibers parallel in one direction determined using eq 5, and E_T is transverse composite modulus (transverse to fiber orientation) calculated using the Halpin−Tsai model (eqs 6 and 7).

$$E_L = V_f E_{l,\text{NFC}} + (1 - V_f)E_m \quad (5)$$

$$E_T = \frac{1 + 2\eta V_f}{1 - \eta V_f} \times E_m \quad (6)$$

$$\eta = \frac{\frac{E_{t,\text{NFC}}}{E_m} - 1}{\frac{E_{t,\text{NFC}}}{E_m} + 2} \quad (7)$$

V_f is the volume fraction of NFC. $E_{l,\text{NFC}}$, $E_{t,\text{NFC}}$, and E_m are NFC longitudinal modulus (84 GPa),[32] NFC transverse modulus (15 GPa),[33] and PCL modulus (0.35 GPa),[34] respectively.

RESULTS AND DISCUSSION

In this work, nanopaper has been grafted with ε-caprolactone by surface-initiated ring-opening polymerization. Filter paper was also grafted in the same manner, as a comparison. The versatility of the present grafting method is demonstrated as the polymerization is performed under normal atmosphere, i.e., in the presence of air, using recently developed titanium based catalysts. For both types of papers, the grafting reactions were run to high and low monomer conversion. This study proposes a new and simple method for nanocomposite preparation based on NFC and shows its potential as a method to develop truly nanostructured materials. Because the polymer is grafted from the nanofibrils, the distribution of the polymer matrix becomes well-controlled.

The polymer grafting generates both grafted and free, unattached, PCL according to Scheme 1. Because titanium-based catalyst does not require any additional co-initiator to catalyze the ROP of ε-CL and subsequently can react with cellulose hydroxyl groups via a trans-alcoholysis reaction, two mechanisms could take place during the reaction. The first one is ROP of ε-CL that is initiated by coordination insertion of the catalyst on the monomer followed by the propagation step that allows the formation of PCL chains on the four arms of the catalyst having equal activity; this mechanism was proposed and proved by Kricheldorf et al.[15] and by others.[16,35] The second mechanism, in situ ROP of ε-CL on cellulose substrates, requires an additional step of initiation where the catalyst is attached to hydroxyl groups of cellulose via trans-alcoholysis

reaction followed by coordination insertion to the monomer and then propagation.

The titanium alkoxides are efficient catalysts for ROP of ε-CL in air according to Parssinen et al.[14] which make them highly interesting alternatives for in situ SI-ROP of ε-CL on cellulose substrates. The nanopaper was prepared according to previous studies and the filter paper (Whatman#1) was chosen for its high cellulose content (>98%) and high purity. Furthermore, Malmström's group has previously reported on the ROP of ε-CL using $Sn(Oct)_2$ as a catalyst from this substrate,[21] therefore it was a suitable comparison in this work. Table 1 summarizes the experiments performed herein.

Table 1. Grafting Reactions from Nanopaper and Filter Paper, Characterization of Free PCL, and Weight Percent of Grafted PCL in the Grafted Cellulose Substrates

sample	reaction time (h)	conv. (%)[a]	$M_{n,th}$ (g/mol)[b]	M_n (g/mol)[c]	PDI	grafted PCL[d] (%)
FP-Ti-33	12.5	33	16 300	10 700	1.16	33
FP-Ti-50	22.0	78	38 600	25 800	2.0	50
NP-Ti-50	19.3	32	15 800	15 000	1.15	50
NP-Ti-64	29.0	70	34 600	27 900	1.45	64
FP-Sn-2	0.4	35	16 500	15 700	1.16	2
FP-Sn-3	0.8	77	36 300	36 700	1.43	3
NP-Sn-61	0.8	45	21 200	20 300	1.13	61
NP-Sn-79	1	81	38 100	39 400	1.59	79
FP-b[e]	22.0	1				4
NP-b[e]	29.0	2				8

[a]Conversion (conv.) determined by ^{1}H NMR signals at 4.05 ($-CH_2O$-, polymer repeating unit) and 4.20 ($-CH_2O-$, monomer). [b]Estimated from the conversion with ^{1}H NMR. [c]Average molecular weight of free polymer determined by chloroform SEC. [d]Percentage of grafted PCL in the grafted cellulose substrate measured by weight difference of the substrate before and after grafting. [e]Blank reaction (without catalyst).

Comparison between High- and Low-Surface-Area Cellulose Substrates. To investigate the grafting ratio, the papers were weighed before and after grafting and the percentage of PCL in the composite was calculated according to the following equation

$$\%\text{grafted PCL} = (WC_{sf} - WC_{si})/WCsf_{sf} \times 100$$

Where WC_{si} is the initial cellulose substrate weight before the reaction and WC_{sf} refers to the weight of the grafted cellulose substrate after purification and drying. The results are presented in Table 1 where the samples are denoted as following: filter paper or nanopaper (FP or NP respectively)-catalyst used for the reaction (titanium (Ti) or tin octoate (Sn)-weight percent of the grafted PCL in the grafted substrate (% grafted PCL). As predicted, the grafted amount of PCL on nanopaper is substantially higher than on filter paper when using $Sn(Oct)_2$ as a catalyst, due to the higher specific surface area of the former. However, and quite surprisingly, this effect was not clearly seen when $Ti(On\text{-}Bu)_4$ was utilized instead (see discussion below). On nanopaper, it was found that 64 wt % PCL could successfully be grafted onto the nanopaper using $Ti(On\text{-}Bu)_4$ in the presence of air and 79 wt % using $Sn(Oct)_2$ under inert atmosphere. This is remarkably high and is expected to reduce moisture sensitivity of the composites. On filter paper, 50 wt % PCL could be grafted using $Ti(On\text{-}Bu)_4$ but only 3 wt % by $Sn(Oct)_2$.

It may be possible to control the composition of the composites by controlling the reaction time although no systematic study has been conducted to demonstrate this.

Comparison between $Ti(On\text{-}Bu)_4$ and $Sn(Oct)_2$. The grafted nanopaper with PCL using $Sn(Oct)_2$ as catalyst (Table 1) shows significantly lower grafting amount of PCL in comparison with grafted filter paper prepared with $Ti(On\text{-}Bu)_4$. One plausible explanation for this is the reaction time and the availability of the OH-groups. Initially, many more OH groups are available on the nanopaper due to its high surface area and with $Sn(Oct)_2$ the reaction is quite fast (<1 h). Under these conditions it could be that the surface-initiated reaction on the filter paper only starts from a few available OH-groups, whereas in nanopaper, it starts from many. However, when $Ti(On\text{-}Bu)_4$ is utilized instead, this reactions takes much longer and the paper is subjected to the reaction solution for up to 22 h. It is possible that during this time and at this elevated temperature (120 °C), the fiber structure of the filter paper disintegrates and more and more OH-groups becomes available during the course of the reaction also for the filter paper, resulting in a much more grafted paper. Moreover, the filter paper becomes more and more hydrophobic during the reaction time which makes it disintegration easier in a hydrophobic media.

A slight delamination of the nanopaper with high amount of grafted PCL could be observed (NP-Ti-64 and NP-Sn-79). This could be explained by a decrease in fiber−fiber interaction due to grafting of a remarkably high amount of hydrophobic polymer to the fibers surface (no mechanical data are available to confirm this).

The characterization of free PCL formed in bulk from ROP of both filter paper and nanopaper (Table 1) show that the number average molecular weight (M_n) of free PCL increased when the conversion (conv.) increased. It should also be noted that the average molecular weight of free PCL obtained with $Sn(Oct)_2$ is almost the same as the theoretical one while the difference between the M_n values and the $M_{n,th}$ is more pronounced with $Ti(On\text{-}Bu)_4$. The less control over the reaction and the difference between $M_{n,th}$ and M_n for titanium *n*-butoxide could be due to its exposure to air for longer time which make its oxidation very probable.

FT-IR Analysis. The extent of the surface-initiated polymerization was investigated by infrared spectroscopy (FT-IR) by observing the peak from the carbonyl group around 1730 cm^{-1} (present in the grafted PCL but absent in cellulose) and two other peaks at 2950 cm^{-1} (CH-stretch) and 3300 cm^{-1} (OH-stretch). The full spectra are presented in the Supporting Information (ESI). Enlargement of the regions 1800−1600 cm^{-1} and 3600−3000 cm^{-1} are represented in Figure 1 along with reference spectra of cellulose and pure PCL.

FT-IR spectra for the grafted cellulose substrates (Figure 1), for both catalysts, show an increase in the intensity of the peak attributed to the carbonyl group at 1730 cm^{-1} in PCL. The intensity of this peak fits well to values of grafting amount in Table 1, i.e., when $Sn(Oct)_2$ has been utilized, a larger signal from the carbonyl peak can be seen for the grafted nanopapers compared to the filter papers and when $Ti(On\text{-}Bu)_4$ has been utilized the difference in grafting amount is more attributed to the higher conversion of the reaction as the peaks are highest for FP-Ti-50 and NP-Ti-64. The other signal that can be utilized to evaluate the grafting is located at 3400−3200 cm^{-1} and assigned to the hydroxyl groups in cellulose. A decrease in this signal indicates that more hydroxyl groups have been used for the SI-ROP and hence, that more PCL is grafted from the

Scheme 1. Proposed Mechanisms of (i) ROP and (ii) in-situ SI-ROP of ε-CL with Ti(O*n*-Bu)$_4$.[15,16]

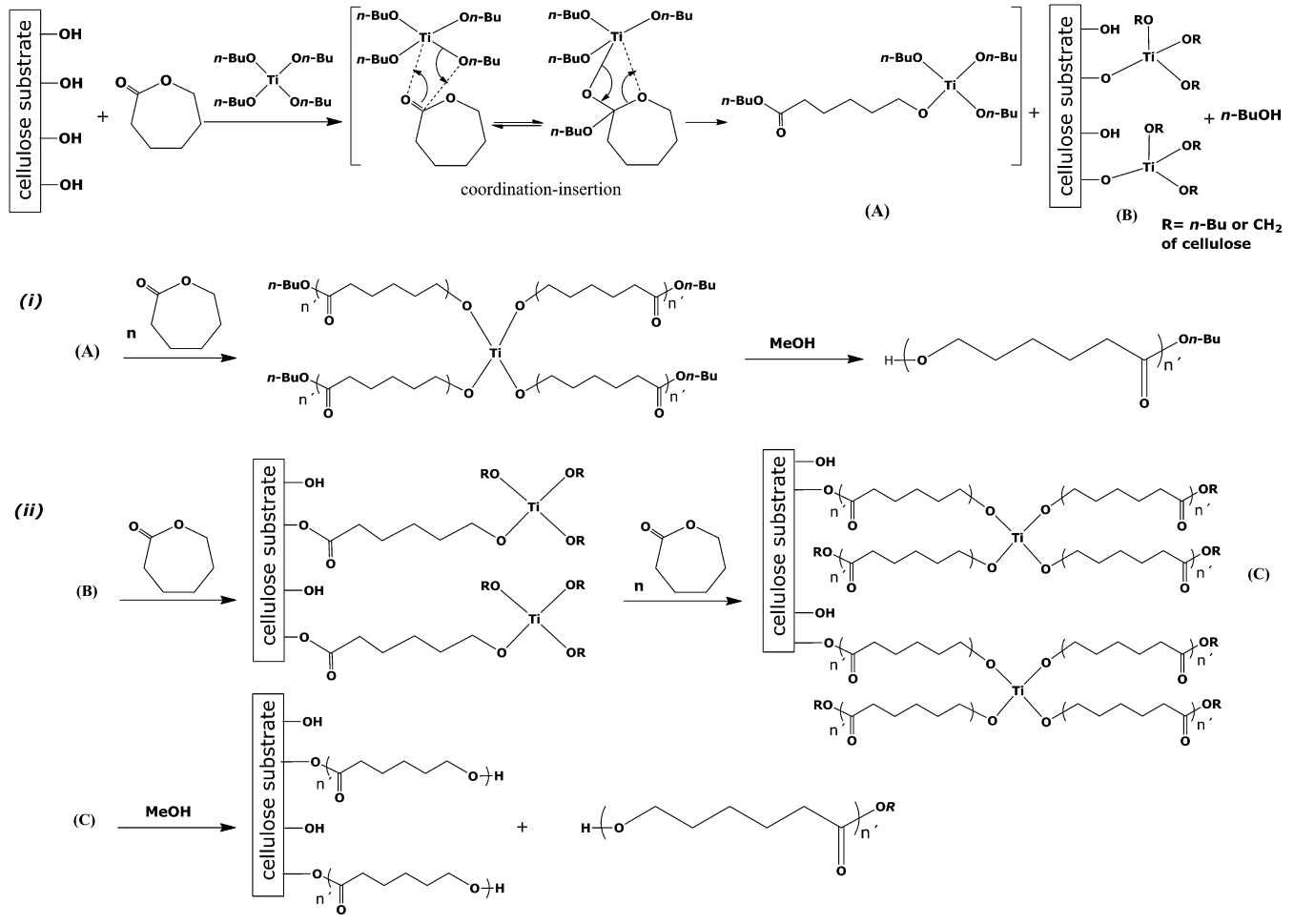

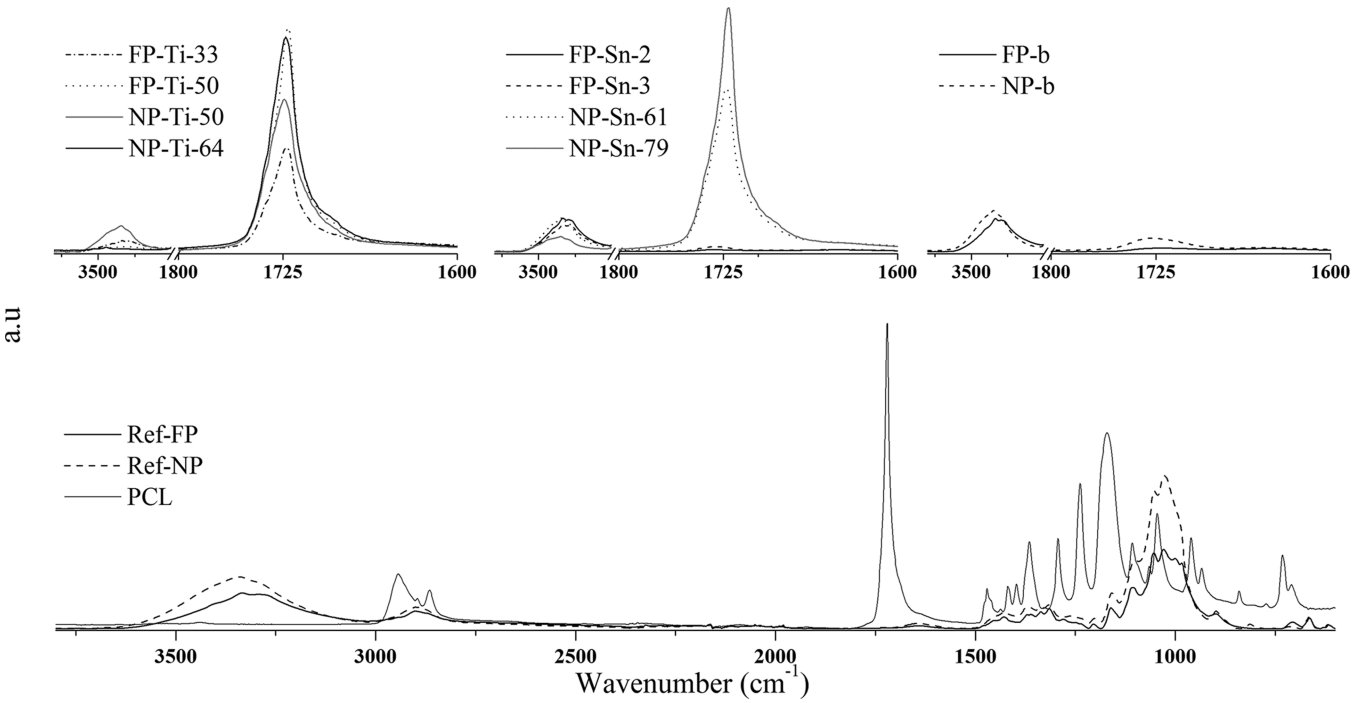

Figure 1. FT-IR spectra of grafted nanopaper and filter paper (enlargement of the regions 1800−1600 cm^{-1} and 3000−3600 cm^{-1}, top) and full spectra of reference PCL and reference cellulose (bottom).

surface of these substrates. Furthermore, the comparison between the signals at 1730 cm^{-1} for grafted nanopaper and grafted filter paper corroborates that the grafting of PCL is higher on nanopaper than on filter paper.

The grafted nanopapers and filter papers were analyzed by DSC (see Table 2) in order to monitor the properties of the

Table 2. DSC Analysis of Grafted Nanopapers and Filter Papers and of Pure PCL

sample	T_c (°C)	T_m (°C)	X_c (%)	M_n (g/mol)
PCL	31.6	56.7	45.9	40 300
FP-Ti-33	27.1	52.9	39.3	10 700
FP-Ti-50	32.6	57.2	47.8	25 800
NP-Ti-50	27.1	51.6	27.7	15 000
NP-Ti-64	30.3	56.0	35.1	27 900
NP-Sn-61	16.6	41.2	19.9	20 300
NP-Sn-79	27.1	53.7	34.7	39 400

polymer grafted. The DSC analysis reveals melting transition between 50 and 57 °C, assigned to melting of the crystalline part of PCL. As predicted, the degree of crystallinity (X_c), the melting temperature (T_m) and the temperature of crystallization (Tc) increase with higher grafting amount (i.e., higher conversion) due to the formation of more grafted PCL on the surface of the cellulose substrates, this is in agreement with results by Lönnberg et al.[21] where a higher T_m and X_c values were obtained for a longer grafted PCL chains. The thermograms are presented in the Supporting Information and results are summarized in Table 2.

The surface structure of the reference and grafted substrates was observed by FE-SEM. The micrographs of reference (ungrafted) filter paper (A) and nanopaper (D) are compared to grafted filter paper (B and C) and grafted nanopaper (E and F) in Figure 2. It is interesting to notice the three orders of

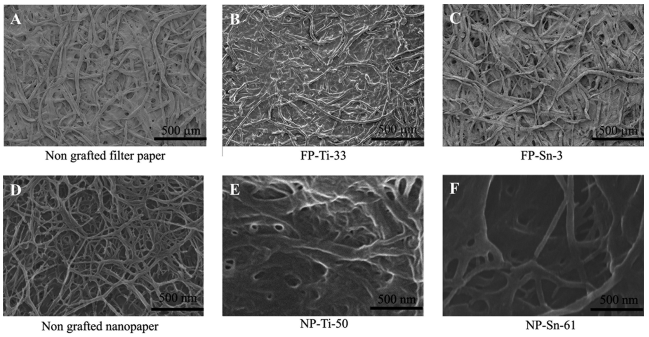

Figure 2. SEM micrographs of (A) nongrafted filter paper and (D) nanopaper, grafted filter paper using (B) Ti(O*n*-Bu)$_4$ and (C) Sn(Oct)$_2$, and nanopaper using (E) Ti(O*n*-Bu)$_4$ and (F) Sn(Oct)$_2$.

magnitude difference between the reference filter paper and nanopaper micrographs. Cellulosic fibers used in the filter paper are typically 5−30 μm, whereas the wood nanofibrillated cellulose is 5−20 nm. The small size of the nanofibrils in the nanopaper is also reflected by its high specific surface area (304 m^2/g, see Table 3). Filter paper, on the other hand, has a surface area of only 0.59 m^2/g (approximately 3 orders of magnitude lower). As can be seen in Figure 2, the grafted samples show a smoother surface texture compared to the reference substrates as the fibers/nanofibers becomes covered with PCL after grafting.

Table 3. BET Specific Surface Area, Pore Size, Porosity, and Density of the Grafted Cellulose Substrates

sample	specific surface area (m^2/g)	pore size (nm)	density (kg/m^3)	porosity (%)
FP-b	0.55	[a]	550	62
FP-Ti-50	0.39	[a]	670	47
ref NP	304	35.8	380	74
NP-Ti-50	52	31.8	600	52
NP-Ti-64	28	28.1	685	47

[a]Out of measurement range of the equipment.

Consequently, the porosity and the specific surface area decreases for the grafted substrates compared to the reference substrates (Table 3 and Figure 3). At 50 wt % of grafted PCL in

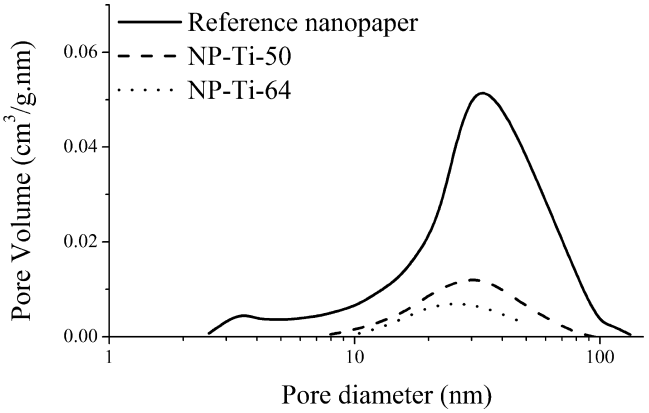

Figure 3. Pore size distribution of nanopaper based on BJH analysis for reference nanopaper (straight line), grafted nanopaper with 50 wt % PCL (dashed line) and with 64 wt % PCL (dotted line).

the nanopaper using Ti(O*n*-Bu)$_4$, the BET is reduced to 52 m^2/g and further to 28 m^2/g at 64 wt % PCL. The pore size of the nanofiber network in the nanopaper also decreases with increasing grafting amount (Table 3 and Figure 3). Ideally, it would be possible to control the pore size of the nanofiber network by controlling the length of PCL chains grafted. This has not been verified in the present paper.

Mechanical properties of the grafted substrates using Ti(O*n*-Bu)$_4$, reference substrates, and the matrix polymers PCL were evaluated by DMA. Results showing storage modulus versus temperature are presented in Figure 4. At room temperature, the reference PCL sample has a storage modulus of 225 MPa. This is relatively low and is due to the glass transition of the PCL being lower than room temperature (∼ −60 °C). Interestingly, the grafted substrates have much higher storage modulus; 700 MPa for the grafted filter paper (FP-Ti-50) and 800 MPa for the grafted nanopaper (NP-Ti-50). The stiffening effect from the nanofiber network is therefore clearly demonstrated. The theoretical modulus value for the NP-Ti-50 composite according to a Tsai-Pagano model (see details in Experimental Procedure section) is 15 GPa. This is much higher than the value from DMA because of presence of 52% porosity (air) in the composites. Starting from 60 °C, the PCL film undergoes an important decrease in the storage modulus of several orders of magnitudes due to PCL melting before it breaks at 75 °C. However, the grafted films retain good mechanical properties at elevated temperature. For example, the storage modulus at 200 °C is 85 MPa for the grafted filter

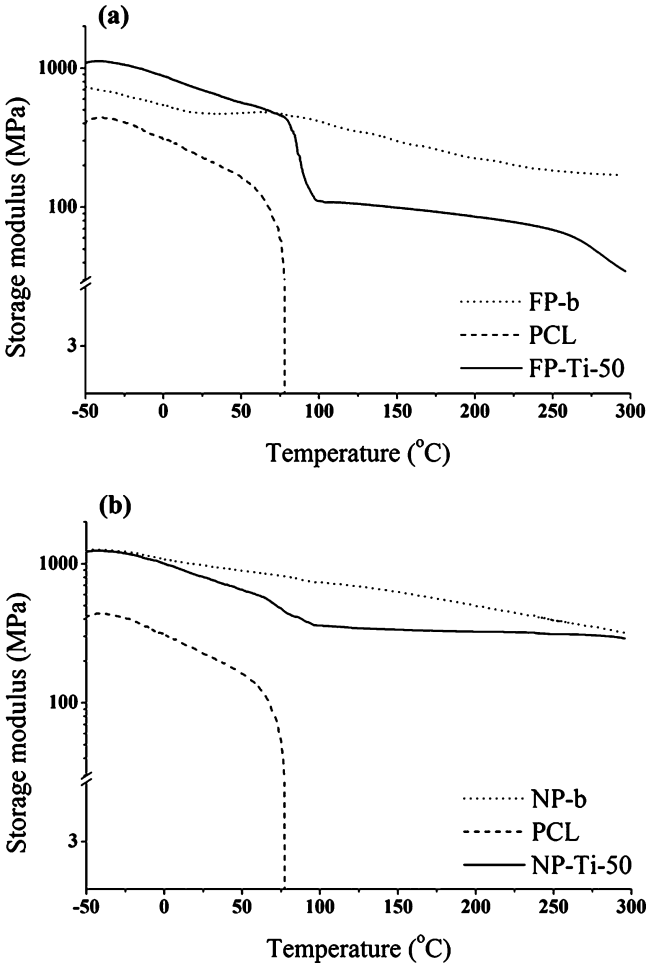

Figure 4. Storage modulus as a function of temperature for the PCL, reference filter paper, and grafted filter paper (left) and for the PCL, reference nanopaper and grafted nanopaper (right).

paper and 325 MPa for the grafted nanopaper. This is due to the mechanical stability of the substrate network as seen from graphs of pure filter paper and nanopaper. This clearly shows the advantage of the present method where a strong and percolated network is used as starting material so that no phase separation could occur during preparation. Such a phase separation would lower the mechanical properties at high temperatures. It should be noted, however, that at higher temperatures (above 200 °C), substrates and grafted samples become brown as a results of cellulose degradation.

The low T_m of PCL gives generally poor creep properties of the PCL based composites. In the present composites, a strong cellulose nanofiber network with numerous interfiber bonds are formed first and this may be advantageous for an improved creep resistance of the corresponding composites.

To compare the mechanical properties of grafted nanopaper and filter paper, DMA results of grafted substrates are shown in Figure 5. These two substrates have similar amount of grafted PCL (50 wt %). Below the melting temperature of the PCL (<75 °C), the mechanical properties are comparable. Above the melting temperature of PCL, the decrease in the storage modulus is more evident for the filter paper compared to the nanopaper, although the later has lower molecular weight PCL grafted. It is expected that the high specific surface area of the nanopaper results in higher contact area between the fibrils compared to the contact area between the fibers thus resulting

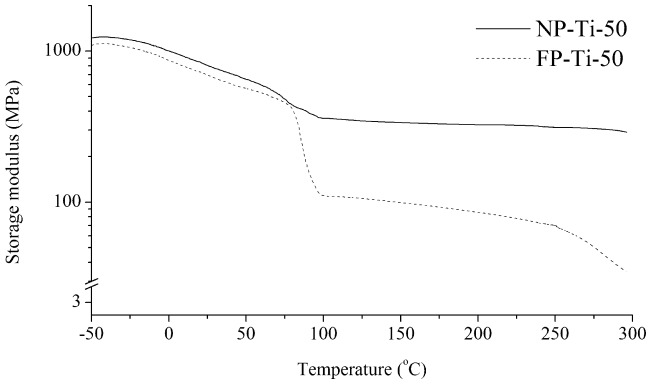

Figure 5. Storage modulus vs temperature of grafted nanopaper (black line) compared to grafted filter paper (dotted line).

in a stronger network resisting higher temperatures. In a composite context, these results show the advantage of nanofiller compared to micrometric filler counterparts.[36]

Although the reference filter paper and nanopaper present good mechanical properties in the whole temperature range studied, their moisture sensitivity considerably reduces mechanical properties at elevated humidities. Moisture uptake for the reference nanopaper and the grafted nanopaper (NP-Ti-50) were evaluated by dynamic vapor sorption (DVS) experiments at three different relative humidities (25%, 50% and 80%). Data are presented in Figure 6. It is found that the

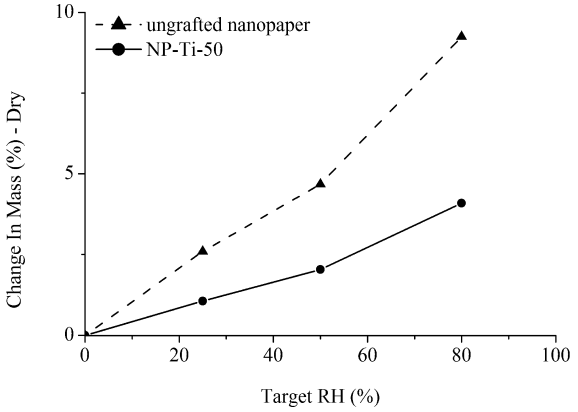

Figure 6. Moisture uptake as monitored by the change in weight of the reference high surface area nanopaper and the grafted nanopaper substrate with 50 wt % PCL (NP-Ti-50).

grafted nanopaper uptake 60% less moisture than the reference nanopaper. This is interesting as the lower water uptake of the composite would result in better performance at elevated humidities compared to the reference cellulosic substrates (no mechanical data available to demonstrate this).

CONCLUSIONS

Cellulose substrates were successfully grafted by in situ surface-initiated ROP of ε-caprolactone using titanium *n*-butoxide as catalyst, which has advantages due to its nontoxicity and that it allows ROP in air, and using the more conventional catalyst tin octoate under inert atmosphere as a comparison. The grafted amount of PCL on nanopaper is significantly higher than on filter paper when tin octoate was utilized as a catalyst according to the results from weight difference before and after the reaction, FT-IR and FE-SEM images. This is due to the high

dx.doi.org/10.1021/am300537h | ACS Appl. Mater. Interfaces 2012, 4, 3191−3198

specific surface area of the nanopaper, allowing more hydroxyl groups to be accessible for the SI-ROP. Moreover, it was shown that tin octoate is an efficient catalyst for the grafting of PCL on nanopaper under inert atmosphere, whereas titanium based catalyst allows SI-ROP of ε-CL in air and leads to high grafting amount of PCL on both cellulose substrates but for longer reaction time compared to tin octoate. In conclusion, this new method for the production of bionanocomposites, starting from an already dried material having high specific surface area and porosity, is a facile route to truly nanostructured composites with high nanofibril content. In the present method, PCL is preferably polymerized from the surfaces of the NFC fibrils. This allows unusual control of the matrix distribution in the composite. Mechanical properties of the composites are far superior to those of pure PCL particularly at elevated temperature because of the percolated and nonaggregated network of the cellulose nanofibrils having numerous fibrils−fibrils joints. The lower moisture uptake of the present composites compared to the reference cellulosic substrate would be advantageous in higher humidity atmosphere where cellulosic substrates are weakened.

■ ASSOCIATED CONTENT

Supporting Information

Thermograms for the DSC measurements and FT-IR spectra. This material is available free of charge via the Internet at http://pubs.acs.org.

■ AUTHOR INFORMATION

Corresponding Author

*E-mail: annac@kth.se (A.C.); houssine@kth.se and Houssine.Sehaqui@empa.ch (H.S.). Tel: +46 8 7908027 (A.C.); +41 587656118 (H.S.). Fax: +46 8 7908283.

Present Address

[⊥]Houssine Sehaqui, EMPA-Materials Science and Technology, Applied Wood Materials laboratory, Überlandstrasse 129, CH-8600 Dübendorf, Switzerland.

Author Contributions

The manuscript was written through contributions of all authors. All authors have given approval to the final version of the manuscript.

Notes

The authors declare no competing financial interest.

■ ACKNOWLEDGMENTS

The Swedish Research Council (VR), the Swedish Research Council Formas, the Swedish Center for Biomimetic Fibre Engineering (BioMime) and Beckers Jubileumsfond are acknowledged for financial support. Anne-Mari Olsson from Innventia AB is thanked for performing Dynamic Vapor Sorption experiments.

■ REFERENCES

(1) Zimmermann, T.; Bordeanu, N.; Strub, E. *Carbohydr. Polym.* **2010**, *79*, 1086−1093.
(2) Henriksson, M.; Henriksson, G.; Berglund, L. A.; Lindström, T. *Eur. Polym. J.* **2007**, *43*, 3434−3441.
(3) Isogai, A.; Saito, T.; Fukuzumi, H. *Nanoscale* **2011**, *3*, 71−85.
(4) Li, W. Y.; Jin, A. X.; Liu, C. F.; Sun, R. C.; Zhang, A. P.; Kennedy, J. F. *Carbohydr. Polym.* **2009**, *78*, 389−395.
(5) Stenstad, P.; Andresen, M.; Tanem, B. S.; Stenius, P. *Cellulose* **2008**, *15*, 35−45.
(6) Lönnberg, H.; Larsson, K.; Lindström, T.; Hult, A.; Malmström, E. *ACS Appl. Mat. Interfaces* **2011**, *3*, 1426−1433.
(7) Siqueira, G.; Bras, J.; Dufresne, A. *Langmuir* **2010**, *26*, 402−411.
(8) Habibi, Y.; Goffin, A.-L.; Schiltz, N.; Duquesne, E.; Dubois, P.; Dufresne, A. J. *Mater. Chem.* **2008**, *18*, 5002−5010.
(9) Lönnberg, H.; Zhou, Q.; Brumer, H.; Teeri, T. T.; Malmström, E.; Hult, A. *Biomacromolecules* **2006**, *7*, 2178−2185.
(10) Hafren, J.; Cordova, A. *Macromol. Rapid Commun.* **2005**, *26*, 82−86.
(11) Tanzi, M. C.; Verderio, P.; Lampugnani, M. G.; Resnati, M.; Dejana, E.; Sturani, E. *J. Mater. Sci.: Mater. Med.* **1994**, *5*, 393−396.
(12) Storey, R. F.; Sherman, J. W. *Macromolecules* **2002**, *35*, 1504−1512.
(13) Labet, M.; Thielemans, W. *Chem. Soc. Rev.* **2009**, *38*, 3484−3504.
(14) Parssinen, A.; Kohlmayr, M.; Leskela, M.; Lahcini, M.; Repo, T. *Polym. Chem.* **2010**, *1*, 834−836.
(15) Kricheldorf, H. R.; Berl, M.; Scharnagl, N. *Macromolecules* **1988**, *21*, 286−293.
(16) Cayuela, J.; Bounor-Legaré, V.; Cassagnau, P.; Michel, A. *Macromolecules* **2006**, *39*, 1338−1346.
(17) Dubois, P.; Krishnan, M.; Narayan, R. *Polymer* **1999**, *40*, 3091−3100.
(18) Priftis, D.; Petzetakis, N.; Sakellariou, G.; Pitsikalis, M.; Baskaran, D.; Mays, J. W.; Hadjichristidis, N. *Macromolecules* **2009**, *42*, 3340−3346.
(19) Lin, N.; Chen, G.; Huang, J.; Dufresne, A.; Chang, P. R. *J. Appl. Polym. Sci.* **2009**, *113*, 3417−3425.
(20) Lönnberg, H.; Fogelström, L.; Berglund, M.; Malmström, E.; Hult, A. *Eur. Polym. J.* **2008**, *44*, 2991−2997.
(21) Lönnberg, H.; Fogelström, L.; Zhou, Q.; Hult, A.; Berglund, L.; Malmström, E. *Compos. Sci. Technol.* **2011**, *71*, 9−12.
(22) Carlsson, L.; Utsel, S.; Wågberg, L.; Malmström, E.; Carlmark, A. *Soft Matter* **2012**, *8*, 512−517.
(23) Labet, M.; Thielemans, W. *Polym. Chem.* **2012**, *3*, 679−684.
(24) Sehaqui, H.; Zhou, Q.; Ikkala, O.; Berglund, L. A. *Biomacromolecules* **2011**, *12*, 3638−3644.
(25) Sehaqui, H.; Zhou, Q.; Berglund, L. A. *Soft Matter* **2011**, *7*, 7342−7350.
(26) Wunderlich, B. *Macromolecular Physics*; Academic Press: New York, 1980, Vol. 3: Crystal Melting, p 363
(27) Brunauer, S.; Emmett, P. H.; Teller, E. *J. Am. Chem. Soc.* **1938**, *60*, 309−319.
(28) Barrett, E. P.; Joyner, L. G.; Halenda, P. P. *J. Am. Chem. Soc.* **1951**, *73*, 373−380.
(29) Sun, C. C. *Int. J. Pharm.* **2008**, *346*, 93−101.
(30) Mark, J. E. *Polymer Data Handbook*; Oxford University Press: Oxford, U.K., 1999.
(31) Agarwal, B. D.; Broutman, L. J. *Analysis and Performance of Fiber Composites*; Wiley: New York, 1990.
(32) Iwamoto, S.; Kai, W.; Isogai, A.; Iwata, T. *Biomacromolecules* **2009**, *10*, 2571−2576.
(33) Diddens, I.; Murphy, B.; Krisch, M.; Müller, M. *Macromolecules* **2008**, *41*, 9755−9759.
(34) Eshraghi, S.; Das, S. *Acta Biomater.* **2010**, *6*, 2467−2476.
(35) Li, P.; Zerroukhi, A.; Chen, J.; Chalamet, Y.; Jeanmaire, T.; Xia, Z. *Polymer* **2009**, *50*, 1109−1117.
(36) Siqueira, G.; Bras, J.; Dufresne, A. *Biomacromolecules* **2009**, *10*, 425−432.